Apoptotic and Necrotic Action Mechanisms of Trimethyltin in Human Hepatoma G2 (HepG2) Cells

ARTICLE *in* CHEMICAL RESEARCH IN TOXICOLOGY · SEPTEMBER 2009

Impact Factor: 3.53 · DOI: 10.1021/tx900120z · Source: PubMed

6 AUTHORS, INCLUDING:

Jiali Cai
Xiamen University
9 PUBLICATIONS **108** CITATIONS
SEE PROFILE

Bowen Li
Fujian Institute of Research on the Structur…
13 PUBLICATIONS **68** CITATIONS
SEE PROFILE

Yixin Chen
Washington University in St. Louis
251 PUBLICATIONS **4,239** CITATIONS
SEE PROFILE

Zhenghong Zuo
Xiamen University
77 PUBLICATIONS **773** CITATIONS
SEE PROFILE

Apoptotic and Necrotic Action Mechanisms of Trimethyltin in Human Hepatoma G2 (HepG2) Cells

Jiali Cai,[†] Mengmeng Wang,[†] Bowen Li,[†] Chonggang Wang,[†,‡] Yixin Chen,[†] and Zhenghong Zuo*,[†,‡]

Key Laboratory of the Ministry of Education for Coast and Wetland Ecosystems, School of Life Sciences, Xiamen University, Xiamen 361005, China, and State Key Laboratory of Marine Environmental Science, Xiamen University, Xiamen 361005, China

Received March 30, 2009

In evaluating the cytotoxic effects and the mechanisms of the apoptotic and necrotic actions of trimethyltin chloride (TMT) on human hepatoma G2 (HepG2) cells, the present study focused on the involvement of antiproliferation, DNA damage, cell death, apoptosis-related proteins, and p53-dependent transcriptional activity. Twenty-four hour TMT treatments (4−64 μM) induced apoptosis and necrosis in HepG2 cells. Thirty-two micromolar and higher concentration significantly increases cell death. DNA damage was observed at 8 μM. Additionally, TMT increased the activity of cellular caspase-3 and the release of mitochondrial cytochrome *c* in a concentration-dependent manner. Our data demonstrated that the Bcl-2 family of proteins was involved in the apoptotic process but that p53 expression level was not affected. The results of luciferase reporter assay indicated that TMT-induced apoptosis seemed to adopt a transcription-dependent route, by activating p53 target genes such as *PUMA* and *p21*.

1. Introduction

Organotin compounds are among the most widely used organometallic compounds. Over the last several decades, organotin compounds have been used in agriculture and industry as biocides, wood preservatives, stabilizers for polyvinylchloride polymers, and antifouling agents (*1, 2*). Trimethyltin chloride (TMT[1]) is one of the most water-soluble organotin compounds. It exists in some polyvinyl chloride products at levels of 8.5−24.9 μg/g (*3*). Polyvinyl chloride pipes are widely used in domestic water systems, and this has contributed to the presence of TMT in drinking water supplies and in the environment. Braman and Tompkins report methyltin (0.49 to 8.1 ng tin/L) in samples of Florida drinking water (*4*). In Canada, methyltin concentrations ranging from 0.5−257 ng tin/L were detected in samples from 10 of 22 houses (*5*). TMT can be absorbed through the respiratory tract, alimentary tract, and skin. Exposure to TMT occurs when workers are exposed to TMT stabilizers, as indicated by urine levels up to 3.75−13.31 μM (*6*). In some countries, TMT does not have commercial application because it is highly toxic, but trace amounts of TMT have been found in the urine of humans not exposed directly to TMT, which reinforces concerns regarding environmental contamination (*7*).

TMT is known as a potent neurotoxicant, which mainly affects the central nervous system. When administered to mammals, TMT causes behavioral alterations such as tremors, seizures, hyperirritability, and learning and memory deficits (*8*). In vitro, TMT appears to have a direct effect on neurons and is often used as a model neurotoxicant for studying neuronal degeneration (*9*) and delayed neuronal cell death (*10*). TMT is also an immunotoxicant, causing splenic atrophy and altered cell division and cell-cycle kinetics in the lymphocytes, resulting in chromosomal alterations and the formation of micrometeruclei (*11*). Furthermore, tri*n*-butyltin (TBT) is shown to induce apoptosis in rat hepatocytes (*12*). A recent study demonstrates that TMT significantly inhibits the rat liver epithelial IAR20 cell growth in a concentration-dependent manner and causes an increase in DNA damage (*13*).

In spite of numerous neurochemical and biochemical studies of TMT, the mechanisms of TMT-induced cell apoptosis and necrosis in vitro remains unknown. It is reported that the liver contains the second highest concentration of TMT, higher than that in the kidney or brain (*14*). In the present study, we chose human hepatoma G2 (HepG2) cells as an in vitro model to investigate the cytotoxicity of TMT and its mechanisms. HepG2 cells retain many of the characteristics of the hepatocytes such as the activities of phase I and phase II enzymes and reflect the metabolism of xenobiotics in the human body better than other metabolically incompetent cells (*15*).

2. Materials and Methods

2.1. Chemicals. TMT, propidium iodide (PI), Hoechst 33342 (HO), methyl thiazolyl tetrazolium (MTT), ethidium bromide (EB), dimethyl sulfoxide (DMSO), normal-melting agarose (NMA), and low-melting agarose (LMA) were purchased from Sigma (St. Louis, MO, USA). All tissue culture supplies were purchased from Hyclone (Logan, UT, USA). Monoclonal antimouse Bcl-2 antibodies, monoclonal antimouse Bax antibodies, monoclonal antimouse cytochrome *c* antibodies, monoclonal antimouse p53 antibodies, polyclonal goat antirabbit β-actin, and enhanced chemiluminescence (ECL) were obtained from Santa Cruz Biotechnology (Santa Cruz, CA, USA). Nitrocellulose membrane (0.2 μm pore size) was

* Corresponding author. Tel: +86-592-2187353. E-mail: zuozhenghong@xmu.edu.cn.
[†] Key Laboratory of the Ministry of Education for Coast and Wetland Ecosystems.
[‡] State Key Laboratory of Marine Environmental Science.

[1] Abbreviations: TMT, trimethyltin chloride; TBT, tri*n*-butyltin; HepG2, hepatoma G2; MTT, methyl thiazolyl tetrazolium; EB, ethidium bromide; DMSO, dimethyl sulfoxide; NMA, normal-melting agarose; LMA, low-melting agarose; ECL, enhanced chemiluminescence; ELISA, enzyme linked immunosorbent assay; Bcl2, B-cell CLL/lymphoma 2; Bax, Bcl2-associated X protein; PI, propidium iodide; HO, Hoechst 33342; PMSF, phenylmethyl sulfonyl fluoride; EGTA, ethylene glycol tetraacetic acid; VDAC, voltage-dependent anion channel; PUMA, p53 upregulated modulator of apoptosis.

10.1021/tx900120z CCC: $40.75
Published on Web 08/06/2009

purchased from Bio-Rad Laboratories (Hercules, CA, USA). All other routine laboratory reagents were obtained from commercial sources and were of analytical grade.

2.2. Preparation of TMT Stock Solution for Experiments. TMT was dissolved in DMSO as a 64 mM stock solution. It was stored at 4 °C, protected from light, and diluted to the final dilution before use. Control cells were treated with the vehicle (DMSO) alone (final concentration 0.1%), which had no detectable effect on the cells.

2.3. Cell Cultures. The HepG2 cell line was obtained from Beijing Xiehe Cell Biology Institute, China. The cells were cultured in Dulbecco's minimal essential medium supplemented with 10% fetal bovine serum, 100 IU/mL penicillin, and 100 μg/mL streptomycin at 37 °C in a humidified atmosphere with 5% CO_2. The cells were harvested with 0.02% EDTA and 0.025% trypsin and then rinsed three times in PBS. The resulting cell suspension was used in following experiment.

2.4. Analysis of Cell Viability. HepG2 cells were harvested during the logarithmic growth phase and then seeded in 96-well plates at a density of 1.5×10^4 cells/mL in a final volume of 190 μL/well, and the cell viability was determined using the conventional MTT reduction assay. This assay is based on the reduction of MTT to formazan, an insoluble intracellular blue product, by cellular dehydrogenases. It provides a sensitive measurement of the normal metabolic status of cells, particularly that of the mitochondria, and it is thus indicative of early cellular redox changes (*16*). The medium containing varying concentrations of TMT was added to the cells, and they were incubated for 24 h. After incubation and treatment with TMT and hydrogen peroxide, cells were treated with 10 μL of MTT (final concentration, 0.5 mg/mL) for 4 h. Dark blue formazan crystals were formed in intact cells. The supernatant was then removed, and the crystals were solubilized with 100 μL of anhydrous DMSO added to each well. The extent of MTT reduction was measured using an ELISA reader (Thermo Electron Corporation Multiskan MK3, USA) at 490 nm with a 570 nm reference filter. Experiments were performed at least three times.

2.5. Detection of Cell Death Using Flow Cytometry. Flow cytometry with the PI/HO was used to distinguish intact, necrotic, and apoptotic cells. This measurement is used to quantify the extent of apoptosis in the total cell population, combining both adherent and floating cells (*17*). Briefly, the cells treated with TMT were washed with ice cold PBS and harvested with 0.02% EDTA and 0.025% trypsin and rinsed three times in PBS; the collected cells were stained with the cell-impermeable dye PI (20 μg/mL) and the cell-permeable dye HO (10 μg/mL) for 15 min in the dark; they were washed twice with PBS; and they were analyzed immediately using Fluorescence Activated Cell Sorter. The data were analyzed using CellQuest software (BD Biosciences, Franklin Lakes, NJ, USA), and 30000 events were analyzed for each independent experiment. Cells were divided into four groups appearing as quadrant I (left and up), quadrant II (right and up), quadrant III (left and down), and quadrant IV (right and down). Cells exhibiting both HO and PI fluorescence, only HO fluorescence, and neither HO nor PI fluorescence were necrotic cells or late apoptotic cells (quadrant II), the early apoptotic cells (quadrant IV), and intact cells (quadrant III), respectively.

2.6. Analysis of DNA Damage Using the Comet Assay. After treatment, aliquots of the cell suspension (50−100 μL, $0.5-1.0 \times 10^5$ cells) were transferred to Eppendorf tubes and centrifuged at 200*g* for 5 min. The supernatant was discarded, and the pellet was mixed in 75 μL of LMA (0.7% in PBS) that was then distributed onto conventional microscope slides, which had been precoated with NMA (0.5% in PBS) and dried at room temperature overnight. After the agarose had solidified (4 °C for 10 min), the slides were immersed in the lysis solution (2.5 M NaCl, 100 mM Na_2EDTA, 10 mM Tris-HCl at pH 10.0, containing freshly added 1% Triton x-100, and 10% DMSO) for 1 h at 4 °C and then placed into a horizontal electrophoresis apparatus filled with freshly made buffer (1 mM Na_2EDTA and 300 mM NaOH, pH 13.0). After 20 min of preincubation (unwinding of DNA), the electrophoresis ran for 40 min at a fixed voltage of 25 V and 300 mA which was adjusted by raising or lowering the level of the electrophoresis buffer in the tank. At the end of electrophoresis, the slides were washed three times with the neutralization buffer (0.4 M Tris-HCl, pH 7.5), stained with 50 μL of EB (20 μg/mL), and kept in a moist chamber in the dark at 4 °C until analysis. All of the above-reported steps were carried out under red light to prevent any additional DNA damage. The cells were analyzed at 100× magnification using a fluorescence microscope equipped with a 50-W mercury lamp (Olympus, Tokyo, Japan). In each experiment, the viability of the cells was determined using the trypan blue method (*18*), and only cultures in which the viability of the cells was ≥80% were analyzed. One hundred fifty randomly selected comet tails [characteristic features resulting from the comet (or single cell gel electrophoresis) assay] from the microscope slides were analyzed using a computerized image analysis system (Komet version 3.1, Kinetic Imaging Ltd., Liverpool, UK) (*19*).

2.7. Analysis of Caspase-3 Enzymatic Activity. The activities of caspase-3 were measured using a Diagnostic Reagent kit purchased from Nanjing Jiancheng Bioengineering Institute (China) according to the manufacturer's instructions. Briefly, samples containing about two million HepG2 cells, which had been treated with different concentrations of TMT for 24 h, were washed with PBS, and then 50 μL of homogenization buffer (250 mM sucrose, 1 mM EDTA, 10 mM sodium pyrophosphate, 10 mM tricine, and 2 mM $MgCl_2$, pH 8.0) was added. Cells were sonicated for 10 s, and the homogenates were centrifuged for 10 min at 12,000*g* at 4 °C. Protein concentration of the supernatants was determined using the Bradford assay (*20*). Caspase-3 assays were carried out using 200 μg of proteins in each microplate with the appropriate protease assay buffer. The appropriate substrate was added, then the microplate was incubated for 4 h at 37 °C. Cleavage of substrates was monitored with an ELISA reader (Thermo electron corporation Multiskan MK3, USA) at 405 nm. Experiments were performed at least three times.

2.8. Western Blot Analysis of the Apoptosis-Related Proteins. The release of mitochondrial cytochrome *c* was determined by Western blot (*21*). Briefly, cells (1.5×10^7 cells/mL) after treatment were washed with PBS and resuspended in ice-cold homogenizing buffer (250 mM sucrose, 20 mM HEPES-KOH (pH 7.5), 10 mM KCl, 1.5 mM $MgCl_2$, 1 mM EDTA, 1 mM EGTA, 1 mM dithiothreitol (DTT), 1 mM phenylmethyl sulfonyl fluoride (PMSF), 1 μg/mL aprotinin, and 1 μg/mL leupeptin). After 30 min of incubation on ice, the cells were homogenized with a glass Dounce homogenizer (30 strokes). The homogenate was initially subject to centrifugation at 14,000*g* for 30 min; supernatants were removed and stored at −80 °C until analysis by gel electrophoresis.

For the Western blot sample preparation, the cell pellet was solubilized in 200 μL of lysis buffer radio immunoprecipitation assay (50 mM Tris (pH 7.4), 150 mM NaCl, 1% Triton X-100, 1% sodium deoxycholate, and 0.1% SDS) containing protease inhibitors (10 mg/mL aprotinin, 10 mg/mL leupeptin, and 1 mM PMSF) and placed on ice for 30 min. After centrifugation at 1000*g* at 4 °C for 15 min to remove debris, the supernatant was carefully recovered. Protein concentrations were determined using the Bradford assay (*20*). All samples were stored at −80 °C prior to electrophoresis.

Supernatant aliquots containing 50 μg or more of proteins were mixed with a 2× volume of sample buffer. The samples were boiled for 5 min and subjected to 12% sodium dodecyl sulfate−polyacrylamide gel electrophoresis. After electrophoresis, the separated proteins were transferred electrophoretically from the gel to nitrocellulose membranes. The membranes were blocked at room temperature for 2 h in PBS buffer containing 5% nonfat dry milk to prevent nonspecific binding of reagents and then incubated with anti-Bcl-2, anti-Bax, anticytochrome *c*, anti-p53, or anti-β-actin at 4 °C overnight. Each antibody was used with a 500-fold dilution. After that, the membranes were washed three times in phosphate buffered saline Tween-20 (PBST) for 15 min and incubated with secondary antibody (1:10000) for 1 h at room temperature. Then the membranes were washed three times in PBST and exposed to 2 mL of ECL reagents for 2 min. Blots were exposed to X-ray film

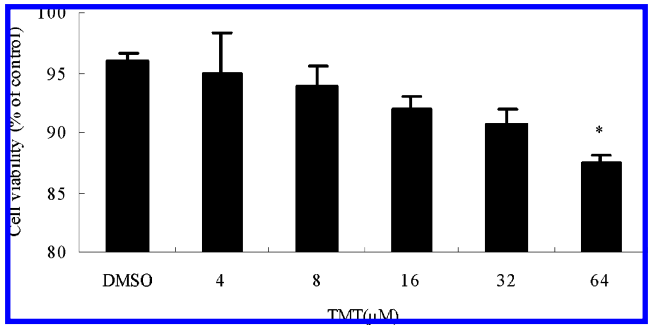

Figure 1. Toxicity of TMT to HepG2 cells. The cells were treated with different concentrations of TMT for 24 h before being subjected to the MTT assay. Values (means ± SD) are data obtained from three independent experiments. Means of exposures with * notation are significantly different at $P < 0.05$.

for 5s for radiographic detection of the bands, and the final exposure time was adjusted by the results of the first exposure. The autoradiograms were scanned and the blots of β-actin, Bcl-2, Bax, cytochrome *c*, and p53 were quantified using densitometry with a Quantity One image analysis system (Bio-Rad Laboratories, Inc., Hercules, CA). The expression levels of Bcl-2, Bax, cytochrome *c*, and p53 were presented as relative expression normalized by β-actin.

2.9. Transient Transfection and Luciferase Reporter Assay. Plasmids of p53-Luc, p21-Luc, pRL-TK, pGL3-Control, and PUMA-FRAG1-Luc were gifts from Professor S.C. Lin (The School of Life Sciences, Xiamen University, Xiamen, China). Transient transfections were carried out using Dosper (Roche, Penzberg, Germany) and LipofectAMINE 2000 (Invitrogen, Carlsbad, CA) according to the manufacturer's instructions. HepG2 cells were transfected in six-well dishes at 90% confluence with different reporters. All of the experiments for luciferase assay were performed using cotransfection of pRL-TK (20 ng) as an internal control. After transfection, the cells were treated with 16 μM TMT for 24 h, and then the luciferase activities of the harvested cells were measured using a luminometer (Berthold Technologies) and a Luciferase Reporter Gene Assay $_{K}$it (Beyotime, China). All transfections were carried out in triplicate at least five times.

2.10. Statistical Analysis. All data were presented as the means ± standard deviation (S.D.). The presence of statistical differences among groups was determined by ANOVA, and the method of least significant difference (Dunnett test) was used to compare the effects between each TMT exposed group and the control. A linear regression was carried out to verify the dose effect. All of the statistical analyses were carried out using the statistical software SPSS 13.0 for Windows. Statistical significance was recognized when $P < 0.05$.

3. Results

3.1. Effect of TMT on HepG2 Cell Viability. An MTT assay was performed to test the effect of TMT on HepG2 cells. As shown in Figure 1, 64 μM TMT significantly reduced the cell viability.

3.2. Detection of Dead Cells Using Flow Cytometry Analysis. Using the HO/PI staining method, we further demonstrated the occurrence of TMT-induced cell death. Representative dot plots of HO/PI staining are shown in Figure 2A. Under control conditions, large numbers of cells were intact live cells. After incubation with different concentrations of TMT for 24 h (especially the 32 μM and 64 μM groups) the populations of intact living cells were decreased, while the numbers of apoptotic and necrotic cells were increased (Figure 2B). The results demonstrate that TMT induced apoptosis and necrosis on HepG2 cells in a concentration-dependent manner.

3.3. Results of the in Vitro Comet Assay Experiment. HepG2 cells were treated with different concentrations of TMT

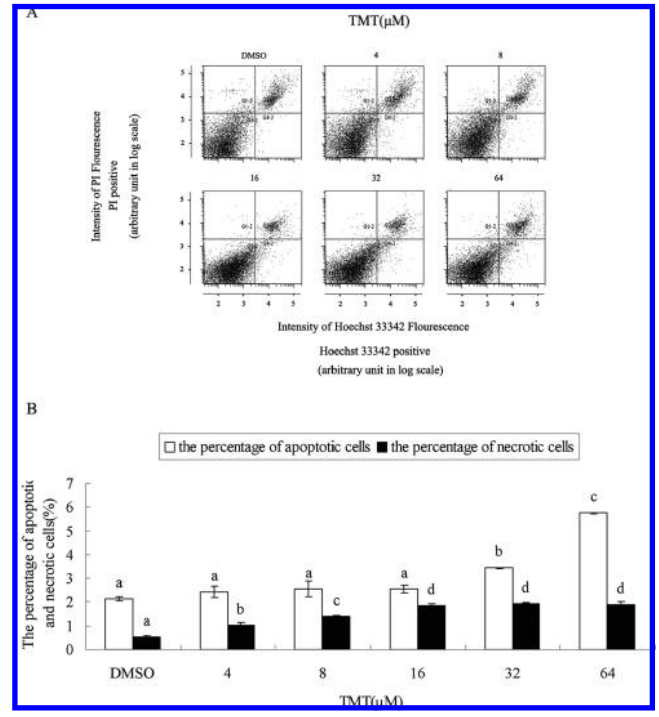

Figure 2. TMT-induced apoptosis and necrosis of HepG2 cells. After incubation with 4−64 μM TMT for 24 h, cells were collected and treated with PI and Hoechst 33342. Samples were analyzed using flow cytometry. The percentages of apoptotic and necrotic cells based on the total cell population analyzed were determined. Values (means ± S.D.) are data obtained from three independent experiments. For each independent experiment, 30000 events were gated. Means of exposures not sharing a common letter are significantly different at $P < 0.05$.

Table 1. Effect of TMT Damage on HepG2 Cells Measured Using the Comet Assay[a]

TMT (μM)	tail length (μm) [b]	tail DNA (%)[b]	tail moment (μm) [b]
DMSO	3.0 ± 1.11 a	0.6 ± 0.24 a	0.02 ± 0.01 a
4	6.5 ± 4.95 a	1.8 ± 1.70 a	0.2 ± 0.22 a
8	15.5 ± 3.54 b	3.8 ± 0.10 a	0.6 ± 0.08 a
16	24.5 ± 0.71 c	12.1 ± 0.14 b	3.0 ± 0.06 a
32	39.0 ± 1.41 d	28.7 ± 3.48 c	11.2 ± 1.25 b
64	61.5 ± 3.53 e	48.6 ± 0.48 d	29.9 ± 3.25 c

[a] Means of exposures not sharing a common letter are significantly different at $P < 0.05$. [b] Values (means ± S.D.) are data obtained from three independent experiments.

for 24 h and harvested for the comet assay; the results are shown in Table 1. Compared with the DMSO control, TMT was shown to cause severe DNA damage in treated HepG2 cells in a concentration-dependent manner as evidenced by the presence of profound comet-like tails of the EB-stained DNA. The results indicated a significant increase in tail length, tail DNA, and tail moment in a concentration-dependent manner.

3.4. Caspase-3 enzymatic activity. When compared to the control group, the activity of caspase-3 increased in a concentration- dependent manner after treatment with TMT (Figure 3). Treatment with 16 μM, 32 μM and 64 μM TMT resulted in a significant increase of the activity of caspase-3 in HepG2 cells.

3.5. Expression of the Bcl-2, Bax, Cytochrome *c*, and p53 in TMT-Treated HepG2 Cells. To further evaluate the mechanism of TMT-induced cell death in HepG2 cells, we examined the expression of apoptosis-related proteins, including p53, the release of cytochrome *c*, Bax, and Bcl-2, using Western blotting analysis (Figure 4A). The results showed that the p53 protein level did not change but that the Bax, Bcl-2, and the release of mitochondrial cytochrome *c* protein levels increased

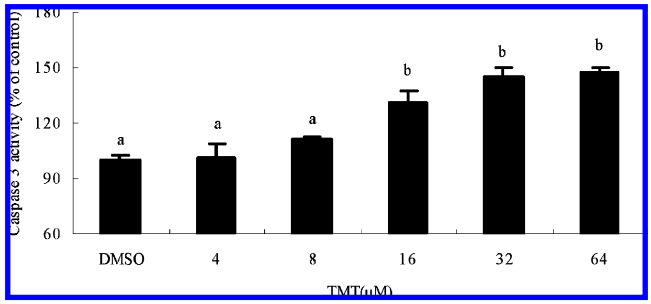

Figure 3. Effect of TMT on caspase-3 enzymatic activity in HepG2 cells. After incubation with 4−64 μM TMT for 24 h, cells were assayed for enzymatic activity. Values (means ± S.D.) are data obtained from three independent experiments. Means of exposures not sharing a common letter are significantly different at $P < 0.05$.

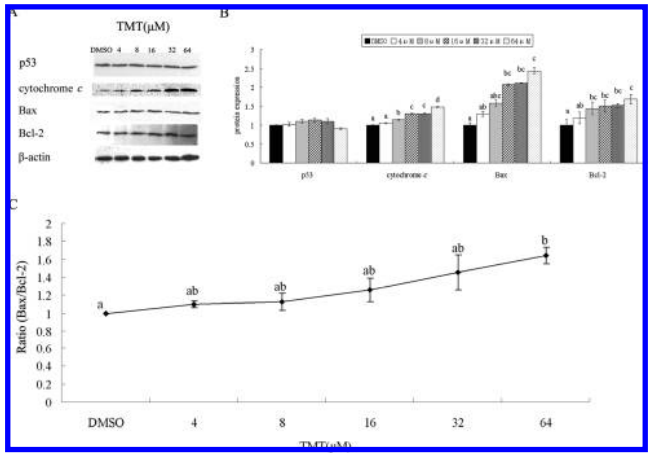

Figure 4. Effect of TMT upon the release of cytochrome *c*, p53, Bax, and Bcl-2 expression in HepG2 cells. Cells were incubated with 4−64 μM for 24 h and collected. (A) A representative autoradiograph of cytochrome *c*, p53, Bax and Bcl-2 expression is shown. (B) Relative expression levels of cytochrome *c*, p53, Bax, and Bcl-2 were obtained on the basis of densitometry. All results are normalized by β-actin. The mean protein expression from DMSO vehicle lysate was designated as 1 in the graph. (C) Results are expressed as the ratio of optical density present in the Bax vs Bcl-2 band. Values (means ± S.D.) are data obtained from three independent experiments. Means of exposures not sharing a common letter are significantly different at $P < 0.05$.

in a concentration-dependent manner (Figure 4B). For cytochrome *c*, the linear regression model revealed a dose-dependent increase with the *R* square 0.86. The result of the Bax/Bcl-2 ratio following TMT treatment is presented in Figure 4C, and it can be seen that the ratio increased significantly, thus shifting the balance toward a preference for apoptosis. The ratio of Bax/Bcl-2 expression also demonstrated a dose response with the *R* square 0.755. These results revealed that the level of some Bcl-2 family proteins was modulated in TMT-induced apoptosis.

3.6. Detection of p53 Transcriptional Activity. When the p53-Luc reporter was introduced into HepG2 cells, luciferase activities did not change (Figure 5), which is in line with the p53 expression levels (Figure 4B). To further explore the exact p53 target genes regulated by TMT, a luciferase activity assay was carried out using two additional reporter genes, PUMA and p21. It was found that treatment with 16 μM TMT stimulated p21-Luc transcription activity more than PUMA-FRAG1-Luc transcription activity (Figure 5).

4. Discussion

Among organotin compounds, TMT is an important environment pollutant. The bioaccumulations of TMT were detected in mollusks and fishes. The levels of TMT in mussel tissue in

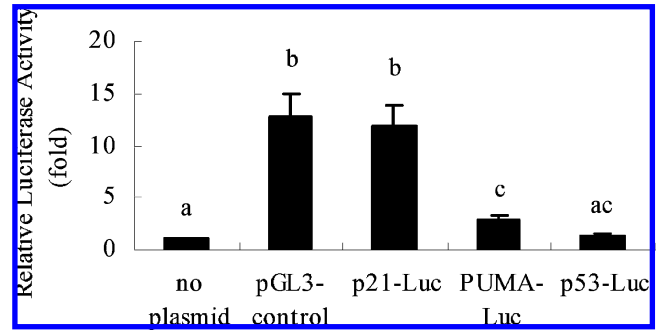

Figure 5. Activation of p53-luciferase reporter gene by TMT. Transfected cells were lysed for luciferase assay 24 h post-transfection. All experiments for the luciferase assay were performed by cotransfection of pRL-TK (20 ng) as an internal control. Values (means ± SD) are data obtained from three independent experiments. Means of exposures not sharing a common letter are significantly different at $P < 0.05$.

the Sado Estuary, Portugal were 5.0−23 ng/g dry wt (*22*), and the seasonal average of trimethyltin in limpets sampled from Turkey estuaries were 0.5−6.90 ng/g dry wt (*23*). The concentration of TMT in eel-pout muscles sampled from the River Elbe and the North Sea in 1993 was 20 ng tin/g fresh mass (*24*). The traces of TMT found in the urine of humans not exposed directly to TMT (*4*) suggested that TMT can possibly accumulate in the bodies of plants and animals and then enter the human body via the food chain and slowly accumulate there.

TMT toxicity in vitro has been examined in a number of cell types, and recent studies indicate that TMT-induced cell death in culture is due to apoptosis or necrosis (*7, 13, 25, 26*). However, most of these studies focused on the effects of TMT on neurons, and there are few reports directly related to the toxic effects of TMT in liver cells. The present study showed that TMT exhibited cytotoxicity on human HepG2 cells in a concentration-dependent manner (Figures 1 and 2) and that there was also a concentration-dependent increase in DNA damage after TMT treatment (Table 1). It is shown that TMT induces apoptosis and necrosis of cerebellar granule cells in vitro at a concentration as low as 0.01 μM (*27*). In the present study, the apoptotic cells did not increase after treatment with 16 μM TMT for 24 h (Figure 2B). It seems that the HepG2 cells are less sensitive to TMT than neuron cell culture, and the insensitivity of HepG2 cells to TMT may result from the tissue selective toxicity of TMT. For example, the protein stannin is known to be important for the toxicity of TMT. Northern blots of rat tissue mRNA revealed that stannin was below the detection levels in the liver (*28*). An antisense oligonucleotide directed against the stannin gene decreased the sensitivity of neuron cluture to TMT (*10*). Considering that the HepG2 cells are liver derived, it is possible that the uncompelling cell death may result from the lack of stannin.

Apoptosis is modulated by complex pathways that involve a series of biochemical regulators and molecular interactions. Although the upstream signaling of apoptosis is obscure, the caspase family of proteases has been shown to play key roles in apoptosis. The apoptotic functions of caspases are involved in both the extrinsic death receptor pathway and intrinsic mitochondrial pathway. Activation of both pathways triggers an amplifying cascade of caspase-3 (*29*), which is a major executioner of apoptotic morphology. Previous studies on TMT-induced neurodegeneration revealed that TMT treament activated caspase-3. Mice exposed to TMT showed an increase of activated caspase-3 in hippocamal neurons (*30*) and neurons in the olfactory bulb and anterior olfactory nucleus (*31*). In the brain of fish, apoptosis was induced as well as caspase-3 activity

by TMT treatments (*32*). Results in our present study showed that caspase-3 was activated by TMT in a concentration-dependent manner, which was highly consistent with the results for the apoptotic rate of the cell exposed to TMT. These correlated changes of caspase-3 and apoptotic rate implied the importance of caspase-3 in the TMT-induced apoptosis on HepG2 cells. The present data showed that TMT induced cytochrome *c* release in a concentration-dependent manner. It is known that mitochondrial cytochrome *c* release from the inner membrane into the cytosol is a common early event in the induction of apoptosis by multiple agents and that cytochrome *c* release is linked to caspase activation and subsequent DNA fragmentation (*33*). According to our data, the increased DNA damage in TMT-treated HepG2 cells was in line with cytochrome *c* release and activation of caspase 3.

In order to further elucidate the molecular mechanism responsible for the TMT-induced apoptosis in HepG2 cells, the expression of Bcl-2 and Bax was analyzed. Both Bcl-2 and Bax belong to the Bcl-2 family, but they have different functions in the apoptosis process (*34*). Increased expression of Bax induces apoptosis, whereas overexpression of Bcl-2 protects cells from apoptosis (*35*). It has also been found that the ratio of Bax to Bcl-2 is important for cell-fate determination (*36*). In the present study, there was obvious up-regulation of Bax expression in HepG2 cells after treatment with TMT. This finding suggested that the effect of the *bax* gene product via the mitochondria might be responsible for the modulation of TMT-induced apoptosis in the HepG2 cells. This result is in line with the fact that TMT induces a concentration-dependent apoptosis in HT-22 cells and rat liver epithelial IAR20 cells by upregulation of Bax protein expression (*13, 37*). One proposed model indicated that Bax translocation to the mitochondrial membrane leads to the formation of a protein complex with the mitochondrial voltage-dependent anion channel (VDAC) (*38*). The Bax−VDAC complex induces opening of the mitochondrial permeability transition pore, which results in mitochondrial membrane potential ($\Delta\Psi$) collapse and subsequent release of apoptosis-promoting factors into the cytoplasm. Conversely, Bcl-2/Bax heterodimer formation may prevent or reduce some of these downstream events (*39*). This finding is in line with our results in TMT-treated cells subsequent to Bax/Bcl-2 ratio increase, cytochrome *c* release, and activation of caspase 3.

p53 plays a critical role in apoptosis after treatment with cytotoxic agents or DNA damage, and it is responsible for regulating cell death through a disruption of the Bax/Bcl-2 equilibrium (*40, 41*). Apoptotic induction by organotins is mediated in a p53-dependent manner, and loss of p53 impairs the release of cytochrome *c* from mitochondria to cytosol (*42, 43*). The results obtained in the present study showed no change in p53 expression levels (Figure 4B), which is consistent with a previous study on TBT-induced apoptosis in human amnion cells (*44*) and TMT-induced apoptosis in rat liver epithelial IAR20 cells (*13*). Their results show that organotin-induced apoptosis may not be mediated by altering the p53 expression levels. To further explore the exact p53 target genes modulated by TMT, a luciferase activity assay was carried out using PUMA and p21 reporters. The results showed that TMT could induce the luciferase activity of p21-Luc and PUMA-Luc. However, TMT could not induce the luciferase activity of p53-Luc, which is in line with its expression levels (Figure 5). The expression of reporter genes indicated an increase of p53-dependent transcriptional activity, while the abundance of the p53 protein did not change. The transcriptional activity of p53 itself can be modulated by a wide array of modifying enzymes and interacting proteins that modify DNA binding preferences and affect the consequences of p53 binding to DNA. An important part of the regulation of p53 transcriptional activity is post-translational modifications including phosphorylation, acetylation, methylation, sumoylation, and neddylation (*45*). Partial or specific acetylation and recruitment of interacing proteins are required in p53-dependent promoter-specific activition on p21 and PUMA (*46*). However, further study is required to explore the actual mechanism. It has been reported that DNA damage often activates the p53-p21 pathway and causes G_1-phase arrest in mammalian cells (*47*). In the present study, treatment with 16 μM TMT for 24 h caused severe DNA damage to HepG2 (Table 1). DNA damage activates the p53-dependent checkpoint pathway that induces the expression of p21, resulting in cell cycle arrest at G1/S transition by inhibition of DNA replication, and the significance of the increased p21 is associated with DNA repair (*48*). The *PUMA* gene encodes two BH3 domain-containing proteins that are localized in the mitochondria (*49*). In response to transactivation by p53, PUMA proteins are induced, which then form a complex with Bcl-2 or Bcl-X_L to induce cytochrome *c* release and cell apoptosis. In the present study, we also found that TMT could induce cytochrome *c* release, in accordance with the induction of the *PUMA* gene by TMT. TMT-induced apoptosis seems to adopt a transcription-dependent route, by activating proapoptotic genes such as *PUMA* and *p21* that are mitochondrial proteins.

In conclusion, the present study demonstrated that TMT could produce apoptosis and necrosis in a concentration-dependent manner in HepG2 cells. The apoptosis appeared to be mediated by the increased expression of Bax, the activity of cellular caspase-3, and the release of mitochondrial cytochrome *c*. Although no obvious change in p53 expression levels was seen, the results of the luciferase reporter assay indicated that TMT-induced apoptosis seemed to adopt a transcription-dependent route, by activating p53 target genes such as *PUMA* and *p21*.

Acknowledgment. This work was supported by the National Key Technology R&D Program of China (2007BAC27B02) and the Natural Science Foundation (40776067) of China. We thank Professor John Hodgkiss for his assistance with English.

Supporting Information Available: Representative images for the comet assay data. This material is available free of charge via the Internet at http://pubs.acs.org.

References

(1) Appel, K. E. (2004) Organotin compounds: Toxicokinetic aspects. *Drug Metab. Rev. 36*, 763–786.
(2) Yonezawa, T., Hasegawa, S. I., Ahn, J. Y., Cha, B. Y., Teruya, T., Hagiwara, H., Nagai, K., and Woo, J. T. (2007) Tributyltin and triphenyltin inhibit osteoclast differentiation through a retinoic acid receptor-dependent signaling pathway. *Biochem. Biophys. Res. Commun. 355*, 10–15.
(3) Gomez, F. D., Apodaca, P., Holloway, L. N., Pannell, K. H., and Whalen, M. M. (2007) Effect of a series of triorganotins on the immune function of human natural killer cells. *Environ. Toxicol. Pharmacol. 23*, 18–24.
(4) Braman, R. S., and Tompkins, M. A. (1979) Separation and determination of nanogram amounts of inorganic tin and methyltin compounds in the environment. *Anal. Chem. 51*, 12–9.
(5) Sadiki, A. I., Williams, D. T., Carrier, R., and Thomas, B. (1996) Pilot study on the contamination of drinking water by organotin compounds from PVC materials. *Chemosphere 32*, 2389–98.
(6) Yanofsky, N. N., Nierenberg, D., and Turco, J. H. (1991) Acute short-term memory loss from trimethyltin exposure. *J. Emerg. Med. 9*, 137–139.
(7) Jenkins, S. M., and Barone, S. (2004) The neurotoxicant trimethyltin induces apoptosis via caspase activation, p38 protein kinase, and oxidative stress in PC12 cells. *Toxicol. Lett. 147*, 63–72.

(8) Ishida, N., Akaike, M., Tsutsumi, S., Kanai, H., Masui, A., Sadamatsu, M., Kuroda, Y., Watanabe, Y., McEwen, B. S., and Kato, N. (1997) Trimethyltin syndrome as a hippocampal degeneration model: temporal changes and neurochemical features of seizure susceptibility and learning impairment. *Neuroscience 81*, 1183–1191.
(9) Philbert, M. A., Billingsley, M. L., and Reuhl, K. R. (2000) Mechanisms of injury in the central nervous system. *Toxicol. Pathol. 28*, 43–53.
(10) Thompson, T. A., Lewis, J. M., Dejneka, N. S., Severs, W. B., Polavarapu, R., and Billingsley, M. L. (1996) Induction of apoptosis by organotin compounds in vitro: Neuronal protection with antisense oligonucleotides directed against stannin. *J. Pharmacol. Exp. Ther. 276*, 1201–1216.
(11) Ghosh, B. B., Talukder, G., and Sharma, A. (1989) Cytotoxic effects of trimethyltin chloride on human peripheral blood lymphocytes in vitro. *Hum. Toxicol. 8*, 349–353.
(12) Jurkiewicz, M., Averill-Bates, D. A., Marion, M., and Denizeau, F. (2004) Involvement of mitochondrial and death receptor pathways in tributyltin-induced apoptosis in rat hepatocytes. *Biochim. Biophys. Acta 1693*, 15–27.
(13) Wang, M., Li, B., Wang, C., Chen, Y., and Zuo, Z. (2008) The concentration-dependent induction of cell death by trimethyltin chloride in rat liver epithelial IAR20 cells. *Toxicol. in Vitro 22* (5), 1136–1142.
(14) Hasan, Z., Zimmer, L., and Woolley, D. (1984) Time course of the effects of trimethyltin on limbic evoked potentials and distribution of tin in blood and brain in the rat. *Neurotoxicology 5*, 217–244.
(15) Knasmuller, S., Parzefall, W., Sanyal, R., Ecker, S., Schwab, C., Uhl, M., Mersch-Sundermann, V., Williamson, G., Hietsch, G., Langer, T., Darroudi, F., and Natarajan, A. T. (1998) Use of metabolically competent human hepatoma cells for the detection of mutagens and antimutagens. *Mutat. Res. 402*, 185–202.
(16) Behl, C., Davis, J. B., Lesley, R., and Schubert, D. (1994) Hydrogen peroxide mediates amyloid beta protein toxicity. *Cell 77*, 817–827.
(17) Mao, W. P., Ye, J. L., Guan, Z. B., Zhao, J. M., Zhang, C., Zhang, N. N., Jiang, P., and Tian, T. (2007) Cadmium induces apoptosis in human embryonic kidney (HEK) 293 cells by caspase-dependent and -independent pathways acting on mitochondria. *Toxicol. in Vitro 21*, 343–354.
(18) Tice, R. R., Agurell, E., Anderson, D., Burlinson, B., Hartmann, A., Kobayashi, H., Miyamae, Y., Rojas, E., Ryu, J. C., and Sasaki, Y. F. (2000) Single cell gel/comet assay: guidelines for in vitro and in vivo genetic toxicology testing. *Environ. Mol. Mutagen. 35*, 206–221.
(19) Jiang, L., Cao, J., An, Y., Geng, C., Qu, S., and Zhong, L. (2007) Genotoxicity of acrylamide in human hepatoma G2 (HepG2) cells. *Toxicol. in Vitro 21*, 1486–1492.
(20) Bradford, M. M. (1976) A rapid and sensitive method for the quantitation of microgram quantities of protein utilizing the principle of protein-dye binding. *Anal. Biochem. 72*, 248–254.
(21) Ghibelli, L., Coppola, S., Fanelli, C., Rotilio, G., Civitareale, P., Scovassi, A. I., and Ciriolo, M. R. (1999) Glutathione depletion causes cytochrome c release even in the absence of cell commitment to apoptosis. *FASEB J. 13*, 2031–2036.
(22) Quevauviller, P., Lavigne, R., Pinel, R., and Astruc, M. (1989) Organotins in sediments and mussels from the Sado estuarine system (Portugal). *Environ. Pollut. 57*, 149–166.
(23) Yemenicioglu, S., Saydam, C., and Salihoglu, I. (1987) Distribution of tin in the Northeastern Mediterranean. *Chemosphere 16*, 429–443.
(24) Shawky, S., and Emons, H. (1998) Distribution pattern of organotin compounds at different trophic levels of aquatic ecosystems. *Chemosphere 36* (3), 523–35.
(25) Figiel, I., and Fiedorowicz, A. (2002) Trimethyltin-evoked neuronal apoptosis and glia response in mixed cultures of rat hippocampal dentate gyrus: A new model for the study of the cell type-specific influence of neurotoxins. *Neurotoxicology 23*, 77–86.
(26) Mundy, W. R., and Freudenrich, T. M. (2006) Apoptosis of cerebellar granule cells induced by organotin compounds found in drinking water: Involvement of MAP kinases. *Neurotoxicology 27*, 71–81.
(27) Gunasekar, P., Li, L., Prabhakaran, K., Eybl, V., Borowitz, J. L., and Isom, G. E. (2001) Mechanisms of the apoptotic and necrotic actions of trimethyltin in cerebellar granule cells. *Toxicol. Sci. 64*, 83–89.
(28) Dejneka, N. S., Patanow, C. M., Polavarapu, R., Toggas, S. M., Krady, J. K., and Billingsley, M. L. (1997) Localization and characterization of stannin: relationship to cellular sensitivity to organotin compounds. *Neurochem. Int. 31*, 801–815.
(29) Fan, T. J., Han, L. H., Cong, R. S., and Liang, J. (2005) Caspase family proteases and apoptosis. *Acta Biochim. Biophys. Sin. 37* (11), 719–727.
(30) Geloso, M. C., Vercelli, A., Corvino, V., Repici, M., Boca, M., Haglid, K., Zelano, G., and Michetti, F. (2002) Cyclooxygenase-2 and caspase-3 expression in trimethyltin-induced apoptosis in the mouse hippocampus. *Exp. Neurol. 175*, 152–160.
(31) Kawada, K., Yoneyama, M., Nagashima, R., and Ogita, K. (2008) In vivo acute treatment with trimethyltin chloride causes neuronal degeneration in the murine olfactory bulb and anterior olfactory nucleus by different cascades in each region. *J. Neurosci. Res. 86*, 1635–1646.
(32) Wang, X., Cai, J., Zhang, J., Wang, C., Yu, A., Chen, Y., and Zuo, Z. (2008) Acute trimethyltin exposure induces oxidative stress response and neuronal apoptosis in *Sebastiscus marmoratus*. *Aquat. Toxicol. 90*, 58–64.
(33) Stridh, H., Kimland, M., Jones, D. P., Orrenius, S., and Hampton, M. B. (1998) Cytochrome c release and caspase activation in hydrogen peroxideand tributyltin-induced apoptosis. *FEBS Lett. 429*, 351–3.
(34) Tsujimoto, Y. (2003) Cell death regulation by the Bcl-2 protein family in the mitochondria. *J. Cell. Physiol. 195*, 158–167.
(35) Cory, S., and Adams, J. M. (2002) The Bcl2 family: regulators of the cellular life-or-death switch. *Nat. Rev. Cancer 2*, 647–656.
(36) Korsmeyer, S. J., Shutter, J. R., Veis, D. J., Merry, D. E., and Oltvai, Z. N. (1993) Bcl-2/Bax: a rheostat that regulates an anti-oxidant pathway and cell death. *Semin. Cancer Biol. 4*, 327–332.
(37) Zhang, L., Li, L., Prabhakaran, K., Borowitz, J. L., and Isom, G. E. (2006) Trimethyltin-induced apoptosis is associated with upregulation of inducible nitric oxide synthase and Bax in a hippocampal cell line. *Toxicol. Appl. Pharmacol. 216*, 34–43.
(38) Shimizu, S., Narita, M., and Tsujimoto, Y. (1999) Bcl-2 family proteins regulate the release of apoptogenic cytochrome c by the mitochondrial channel VDAC. *Nature 399*, 483–487.
(39) Zha, H., and Reed, J. C. (1997) Heterodimerization-independent functions of cell death regulatory proteins Bax and Bcl-2 in yeast and mammalian cells. *J. Biol. Chem. 272*, 31482–31488.
(40) Mihara, M., Erster, S., Zaika, A., Petrenko, O., Chittenden, T., Pancoska, P., and Moll, U. M. (2003) p53 has a direct apoptogenic role at the mitochondria. *Mol. Cell 11*, 577–590.
(41) Vogelstein, B., Lane, D., and Levine, A. J. (2000) Surfing the p53 network. *Nature 408*, 307–310.
(42) Hoti, N., Zhu, D. E., Song, Z., Wu, Z., Tabassum, S., and Wu, M. (2004) p53-dependent apoptotic mechanism of a new designer bimetallic compound tri-phenyl tin benzimidazolethiol copper chloride (TPT-CuCl2): in vivo studies in Wistar rats as well as in vitro studies in human cervical cancer cells. *J. Pharmacol. Exp. Ther. 311*, 22–33.
(43) Tabassum, S., and Pettinari, C. (2006) Chemical and biotechnological developments in organotin cancer chemotherapy. *J. Organomet. Chem. 691*, 1761–1766.
(44) Zhu, X., Xing, M., Lou, J., Wang, X., Fu, W., and Xu, L. (2007) Apoptotic related biochemical changes in human amnion cells induced by tributyltin. *Toxicology 230*, 45–52.
(45) Millau, J. F., Bastien, N., and Drouin, R. (2009) P53 transcriptional activities: a general overview and some thoughts. *Mutat. Res. 681* (2−3), 118–33.
(46) Kruse, J. P., and Gu, W. (2009) Modes of p53 Regulation. *Cell 137*, 609–622.
(47) He, G. G., Siddik, Z. H., Huang, Z. F., Wang, R. N., Koomen, J., Kobayashi, R., Khokhar, A. R., and Kuang, J. (2005) Induction of p21 by p53 following DNA damage inhibits both Cdk4 and Cdk2 activities. *Oncogene 24* (18), 2929–2943.
(48) Sheikh, M. S., Chen, Y. Q., Smith, M. L., and Fornace, A. J. (1997) Role of p21Waf1/Cip1/Sdi1 in cell death and DNA repair as studied using a tetracycline-inducible system in p53-deficient cells. *Oncogene 14*, 1875–1882.
(49) Li, Q. X., Wang, X., Wu, X. L., Rui, Y. N., Liu, W., Wang, J. F., Wang, X. H., Lion, Y. C., Ye, Z. Y., and Lin, S. C. (2007) Daxx cooperates with the Axin/HIPK2/p53 complex to induce cell death. *Cancer Res. 67*, 66–74.

TX900120Z